Exploiting Extraordinary Optical Transmission in Plasmonic Slit Nanoantennas for Sensor Applications

Ricardo A. Marques Lameirinhas ⬡, *Graduate Student Member, IEEE*, Catarina P. Correia V. Bernardo ⬡,
João Paulo N. Torres ⬡, António Baptista ⬡, *Member, IEEE*, and Maria João M. Martins ⬡

Abstract—In this article, a plasmonic gold nanoantenna is proposed as a sensor to monitor refractive index variations between 1.30 and 1.35. These values are defined since they are characteristic of, for instance, water-based solutions, DNA, or haemoglobin. To simulate the device a novel model is used, which takes advantage of the wave-particle dualism and the generalised Fresnel coefficients for absorbing media. Although it is a time-domain model, in this research work the model is improved to compute steady state and frequency-domain results. The response to a Dirac excitation is obtained using that novel model. The steady state is reached for a long pulse emission. The long pulse emission is emulated by a Dirac comb and consequently, the optical response of the device for this kind of excitation is obtained considering the sum of several Dirac's responses shifted in time. Then, steady state might be reached as suggested by the presented results. Taking into account the obtained pulse responses, the refractive index sensor for the range 1.30–1.35 is proposed. The obtained results suggest that 350 nm and 450 nm are the best wavelengths to detect these analyte variations. The sensitivity reaches values up to around 110%/RIU, but sensitivities around 80%/RIU are computed within the range 250–500 nm.

Index Terms—Extraordinary optical transmission, nanoantennas, nanostructures, optical devices, optics, plasmonics, sensors, subwavelength structures, surface plasmon polaritons.

I. INTRODUCTION

NANOTECHNOLOGIES are nowadaysptpt an important research field, where some outstanding phenomena have been discovered which are useful, for instance, in the development of nano-sensors with excellent sensitivities and quite small dimensions.

In 1998, Ebbesen reported radiation spectra of metallic nanoarrays with values higher than those predicted by classical theories, calling this phenomenon Extraordinary Optical Transmission (EOT) [1]. He emphasised that its main agents were Surface Plasmon Polaritons (SPP) [1]. However, this was only proven in 2006 by Lalanne and Hugonin [2]. This type of device is called nanoantennas due to their ability to concentrate and locally amplify radiation.

The reason why classical theories fail to predict EOT is because they do not consider propagation in the metal in the form of evanescent waves [3], [4], [5], [6]. They assume that the metal is opaque and perfectly conducting, reflecting all radiation. However, in the optical spectral region, the radiation penetrates the metal within a distance in the order of tens to hundreds of nanometres [3]. Thus, not all the radiation is reflected. Moreover, if the device has dimensions of the order of these nanometres of penetration distance, then the radiation can reach another interface, enabling transmission through the metal [5], [7].

The use of nanoarrays as sensors has been studied [3], [4], [5], [6]. Their working principle is based on the fact that SPP resonances vary according to the refractive indices of the media at a given interface. Considering that one of these media is a metal and the other is an analyte/sample, a sensor can be designed if: the refractive index of the sample varies with a given stimulus and the index of the sample is known before the stimulus, or if a given sample is used as a reference and another is unknown. It produces an optical intensity variation in the detector and, measuring that, it is possible to determine the refractive index and therefore identify the unknown sample from among those hypothesised.

This working principle is general to SPP-based sensors. However, nanoantennas have the great advantage of concentrating the radiation, thus requiring smaller detectors. In the same sense, compared to Kretschmann or some optical fibre-based sensors, nanoantennas make it possible to miniaturise the entire sensor, a useful advantage for real-time and in-vivo analysis. In addition, nanoantennas are a more complex device with multiple interfaces. Compared to these other types of sensors, there are a greater number of variables, i.e. degrees of freedom for designing the sensor, namely the thickness of the layers (the only geometric variable in the Krestchamnn's structure), the dimensions and shapes of the slits/apertures. On the other hand, while Kretschmann's sensors tend to be considered for a monochromatic emitter that is very focused on the material, in the case of nanoantennas a larger spectral region and the incidence of a plane wave can be considered.

A novel model based on the generalised Fresnel coefficients and on the wave-particle dualism was proposed, overcoming

Ricardo A. Marques Lameirinhas and Catarina P. Correia V. Bernardo are with Instituto Superior Técnico, 1049-001 Lisboa, Portugal, and also with Instituto de Telecomunicações, 1049-001 Lisboa, Portugal (e-mail: ricardo.lameirinhas @tecnico.ulisboa.pt; catarina.bernardo@tecnico.ulisboa.pt).

João Paulo N. Torres is with the Instituto de Telecomunicações, 1049-001 Lisboa, Portugal, and also with the Academia Militar/CINAMIL, 1169-203 Amadora, Portugal (e-mail: joaoptorres@hotmail.com).

António Baptista is with Instituto Superior Técnico, 1049-001 Lisboa, Portugal (e-mail: baptista@tecnico.ulisboa.pt).

Maria João M. Martins is with Academia Militar/CINAMIL, 1169-203 Amadora, Portugal (e-mail: mariajoaomartins2@gmail.com).

Digital Object Identifier 10.1109/JPHOT.2024.3376641

these limitations and bringing more geometric intuition [3], [4], [5], [6]. Taking advantage of this, a biosensor based on nanoantennas exploiting EOT is proposed in this article. The sensor aims to detect refractive index variations around 1.33, namely to distinguish analytes with refractive index of 1.30, 1.33 and 1.35.

This refractive index range has tremendous importance since 1.33 is the water's refractive index. For that reason, the refractive index of water-based samples will vary around these values. For instance, to monitor the sugar (e.g.: glucose) or salt concentration in water or water-based solutions (e.g.: blood) [8], [9], to distinguish water-based solutions and some other liquids [10], monitor haemoglobin and blood [11], [12], several protein and DNA solutions [13], [14], [15], [16], [17], [18], [19], [20], [21].

II. METHODOLOGY

A model based on the Fresnel equations and wave-particle dualism has been proposed to analyse this type of problem [3], [4], [5], [6].

The typical Fresnel equations are not valid since they are deduced for lossless media and are typically used in media with weak losses. In previous and recent works, they were generalised, based on Maxwell's theory [3], [4], [22], [23]. Using this approach, the optical paths are completely defined and the radiation propagation and its interactions in interfaces can be described with increased detail [3], [4], [5], [6], [22], [23]. On top of these advantages, the model allows an improved geometrical interpretation which is important for the theoretical understanding of this phenomenon and its application in the design of sensors.

The methodology considers inhomogeneous waves, being $\hat{e}$ the normal to the plane of constant phase, and $\hat{g}$ the normal to the plane of constant amplitude. Generically, there is no coincidence between them. If it happens, the wave is defined as homogeneous. There is an angle θ for the real component of the wavevector (normal to the equi phase planes) and an angle ψ representative of its imaginary part (normal to the equi amplitude planes) [3], [4], [5], [6], [22], [23].

The wavevector is complex as presented in expression 1, being $\hat{s}$ the interface normal vector and k_0 the wavevector in vacuum. N and K are the apparent refractive index components, which are related to the complex refractive index $\bar{n} = n + jk$ [3], [4], [5], [6], [22], [23].

$$\bar{k} = k_0 \left(N\hat{e} + jK\hat{g} \right) \tag{1}$$

The relation $R + T - M + L = 1$ is valid at the interface and it is determined by the energy conversation law. There, R is the reflection power coefficient, T is the transmission power coefficient, L is the interface losses power coefficient and M is a correction coefficient due to wave interference at the interface. Expression set 2 presents the expressions to determine all the coefficients, where ϵ_0 is the vacuum electrical permittivity, ω the angular frequency and σ_s electrical conductivity at the surface/interface. In most cases $\sigma_s \to 0$, since because the power loss at the interface is lower in comparison with the media absorption, given by expression 3 [3], [4], [5], [6], [22], [23]. The expressions are for TM waves, and the subscript i and t are
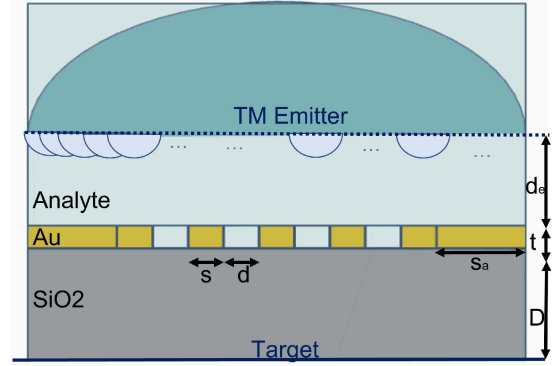

Fig. 1.   Nanoantenna illustration.

respectively for the incident and transmission media.

$$\begin{cases} R_p = \left| \dfrac{\bar{n}_t^2 \bar{k}_i - \bar{n}_i^2 \bar{k}_t + \sigma_s \bar{k}_i \bar{k}_t / (\omega\epsilon_0)}{\bar{n}_t^2 \bar{k}_i + \bar{n}_i^2 \bar{k}_t + \sigma_s \bar{k}_i \bar{k}_t / (\omega\epsilon_0)} \right|^2 \\[2mm] T_p = \left| \dfrac{2\bar{k}_i / \bar{n}_i^2}{\bar{k}_i / \bar{n}_i^2 + \bar{k}_t / \bar{n}_t^2 + \sigma_s \bar{k}_i \bar{k}_t / (\omega\epsilon_0)} \right|^2 \dfrac{Re\{\bar{k}_t / \bar{n}_t^2\}}{Re\{\bar{k}_i / \bar{n}_i^2\}} \\[2mm] M_p = Im\left\{ \dfrac{\bar{n}_t^2 \bar{k}_i - \bar{n}_i^2 \bar{k}_t + \sigma_s \bar{k}_i \bar{k}_t / (\omega\epsilon_0)}{\bar{n}_t^2 \bar{k}_i + \bar{n}_i^2 \bar{k}_t + \sigma_s \bar{k}_i \bar{k}_t / (\omega\epsilon_0)} \right\} \dfrac{Im\{2\bar{k}_i / \bar{n}_i^2\}}{Re\{\bar{k}_i / \bar{n}_i^2\}} \end{cases} \tag{2}$$

$$A = e^{-k_0 \, K\cos(\alpha)d} \tag{3}$$

In the developed novel model, photons are generated with a given direction and characterised by a wavevector. Each photon is an object in an object-oriented program, moving in media according to its coordinates. Their movement through the media is described by Maxwell's equations, which in this case is the same as saying that they change at the interfaces based on Fresnel coefficients and the generalised laws of refraction and reflection.

Since photons represent a quantum of light, they can not be divided and consequently on the interface they will be either reflected or refracted. The reflection probability at the interface is $P_{reflected} = R$ and the refraction one $P_{refracted} = T - M$.

This semi-classical, semi-analytic and time-domain model is used to evaluate the performance of a plasmonic slit nanoantenna as a sensor, exploiting EOT. The details about the model are in [3], [4], [5], [6], where it is proposed and validated.

The model is implemented in Python, emulating a TM wave based on the Huygens-Fresnel principle by considering a total of 250 point sources distributed along a line. Each point source is characterised by 720 optical paths, one per $0.5°$. Photons are emitted following Poissonian distribution in each optical path, considering the average emission of one photon per optical path. As illustrated in Fig. 1, parallel to the emission line is a gold nanoantenna, composed of 4 slits of $d = 155$ nm, separated by $s = 155$ nm and with $t = 30$ nm of thickness. The nanoantennas have also a metal extension of $s_a = 1000$ nm on both sides. The emission line and the gold nanoantenna are distanced by $d_e = 155$ nm, considering the media as the analyte one. The nanoantenna is on top of a quartz layer, there a target (detector) is placed $D = 1550$ nm away from its rear. These parameters are defined based on previous studies and to have balanced between metal (sensitivity) and transmitted power [3], [4], [5], [6], [7].

This research work aims to analyse the possibility to design a slit plasmonic nanoantenna to act as a sensor, namely to
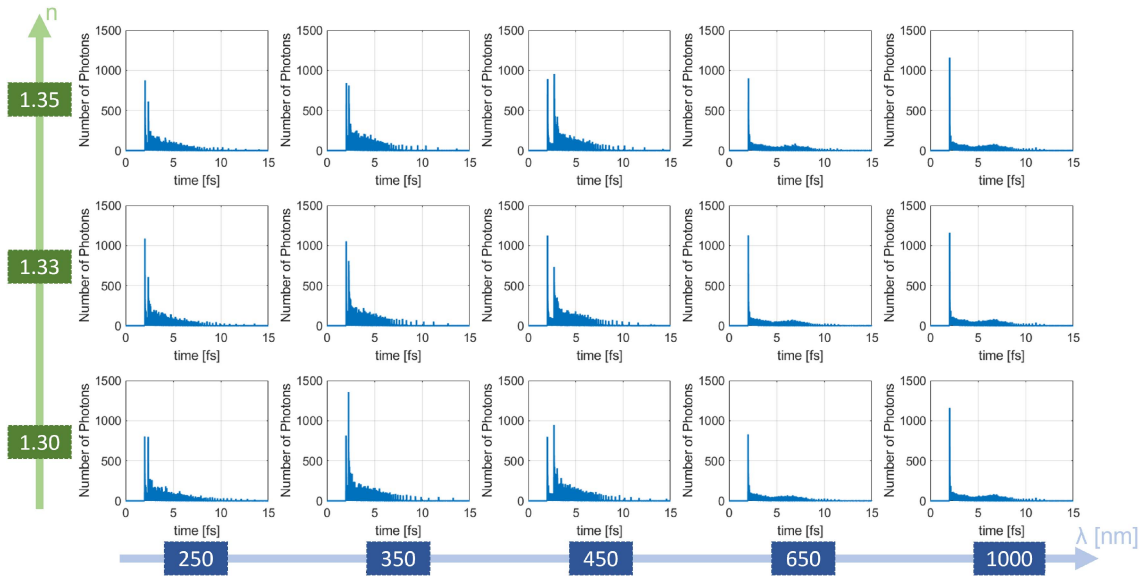
Fig. 2.   Time responses of the gold nanoantenna for several wavelengths and analyte's refractive indexes considering a Dirac excitation.

detect variation in the refractive index of a certain medium. Furthermore, it is intended to verify the influence of EOT in such responses.

To achieve this goal, the time domain response of a four-slit nanoantenna is obtained and compared considering an analyte's refractive index variation between 1.30 and 1.35 and a Dirac emission with a time resolution of 3.3×10^{-18} s. The quartz optical properties are modelled by Gao's model, where the gold's refractive index is characterised by Rakic's Drude-Lorentz model [24]. According to experimental evidences, electrical permittivity values can characterise these materials at nano-dimensions: "below 10–20 nm, the classical theory deteriorates progressively due to its neglect of quantum effects such as nonlocality, electronic spill-out, and Landau damping" [25]. The materials' characterisation by the complex electrical permittivity remains valid, since there are significant atoms: the gold atom has a dimension of 0.146 nm with a lattice constant of about 0.407 nm.

A new methodology approach is used to describe the steady state response of the device. This regime is reached when emitting a long pulse. Since time is discrete in the implemented model, the pulse is generated as a Dirac comb, where the time distance between pulses is very small compared with the time response of the material. Thus, the pulse response is the sum of time-domain responses shifted in time. For each emitted Dirac, the response is assumed to be the same and the long pulse response is the sum of all the Diracs' responses shifted accordingly to its emission time.

III. RESULTS

A. Dirac Time Responses

The time response of the gold nanoantenna is presented in Fig. 2 for different wavelengths and for different analyte refractive indexes. At a wavelength of 1000 nm the response has a low

refractive index dependence since metals reflect all the radiation. However, in the optical range surface plasmon polaritons may be excited in the analyte-metal interface and propagate inside the metal. Thus, there is some energy that might be transmitted through the metal layer, reaching the target. In these cases, the device is working at resonant wavelengths, which are according to previous analysis [3], [4]. For that reason, the number of photons in the target is increased but at different time stamps. Besides the optical paths that pass on the slits, there are others that pass inside the metal that reach the target. However, the energy velocity is different and consequently, other peaks appear in the time response. The responses at wavelengths of 350 nm and 450 nm present a huge number of extraordinary photons, the ones that pass through the gold, which in accordance with previous analysis [3]. Also, the time response in Fig. 2 varies with the analyte's refractive index value.

Fig. 3 shows how the number of photons varies for different wavelengths, considering the Dirac excitation. First, the number of photons incident on the nanoantenna tends to be constant, and the small fluctuations are due to the distribution of photons in the emitter (considered as noise). Then, it is possible to verify that in the resonance influence region, the number of photons absorbed in the metal is greater than the number of photons detected. The number of photons absorbed and the number of photons detected that have passed through the metal tend towards zero. However, it is verified that in the entire visible spectrum the metal absorbs photons, that is, although for longer wavelengths the reflection of the metal tends to be total, the photons that manage to enter the metal cannot leave it and end up being absorbed. For wavelengths in which the number of photons detected due to EOT is zero, it is found that the detected intensity is the same, i.e., it considers the number of photons passing through the aperture which tends to be constant, since the metal reflects a lot (more than 90%). This value tends to be the same for all wavelengths outside the region of influence of the resonances and for the
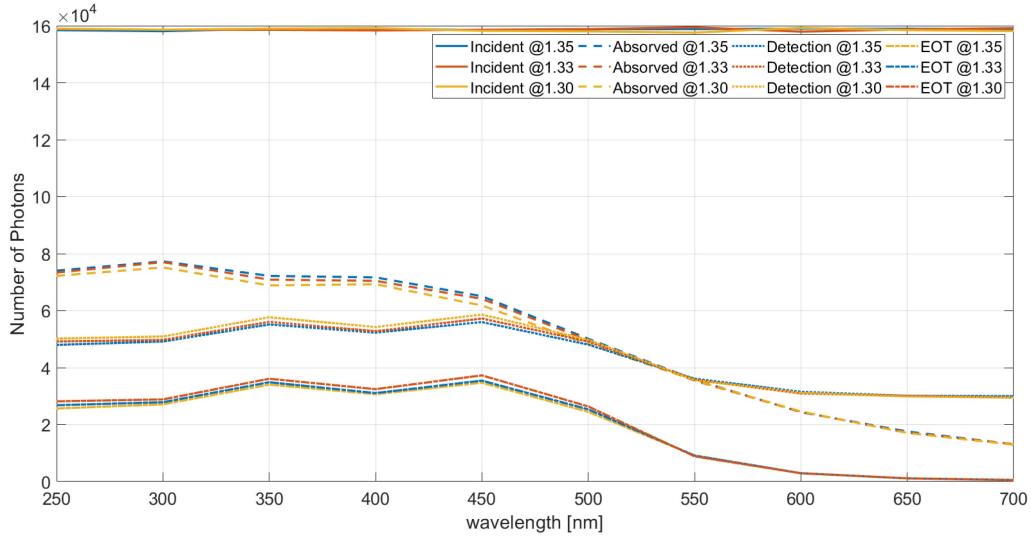
Fig. 3. Number of photons incident, absorbed (in the metal), detected and detected that passes through the metal.
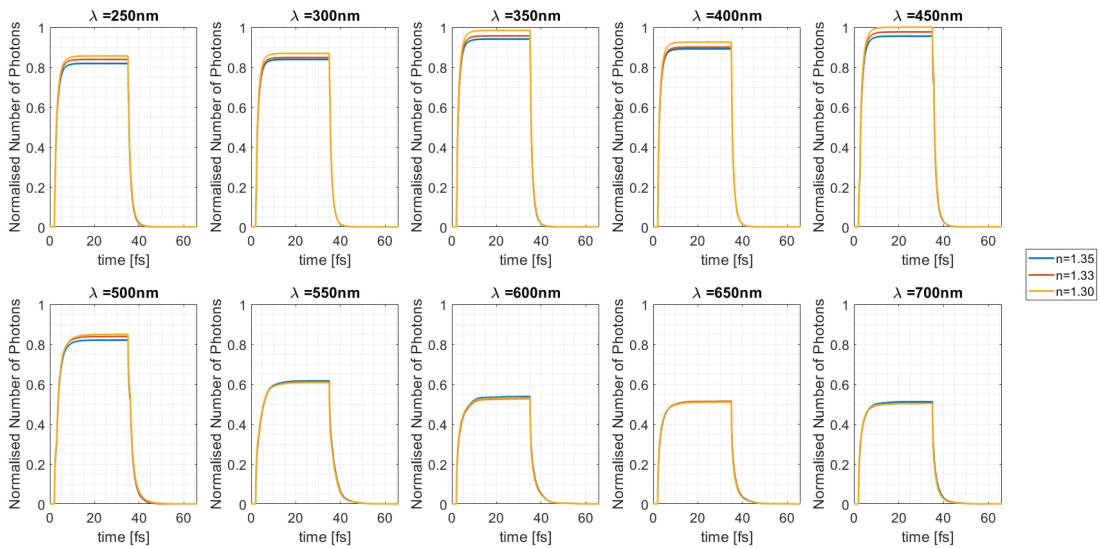

Fig. 4. Normalised time responses of the gold nanoantenna for several wavelengths and analyte's refractive indexes considering a pulse excitation.

samples considered (the device tends to have zero sensitivity). Within the region of influence of the resonances, the detected photons pass mostly through the metal. In this way, it will be possible to have sensitivity due to the resonances in the analyte-gold interfaces. The shape of the detected spectrum is identical to the number of detected photons that have passed through the metal. There is only one offset associated with the photons passing through the slits and not hitting a single nanoantenna's interface.

B. Steady State and Spectral Responses

A Dirac comb is used to emulate the response to a constant emission. Considering the device response as time-invariant, its response to a constant emission is the sum of the Dirac responses shifted in time. Then, using the time-domain semi-classical

model is also possible to extrapolate results in the frequency domain, analysing the response in its steady state.

Fig. 4 presents the results of a Dirac comb excitation, where Diracs are emitted with a time interval equal to the time resolution and with a comb's duration of approximately 33 fs. Results are taken in the optical range, namely in the ultraviolet-visible spectral regions, within a wavelength range from 250 nm to 700 nm, using steps of 50 nm. Fig. 4 illustrates the number of photons that reached the target at a certain time. The values are normalised to the maximum, which is obtained at 450 nm for an analyte's refractive index of 1.30.

For wavelengths outside the gold SPP resonances, it is verified that the obtained number of photons is half the maximum value. The response maximum tends to decrease as analysed starting at 450 nm to 700 nm. Furthermore, another resonance is near 350 nm, so that the pulse response presents a local maximum.
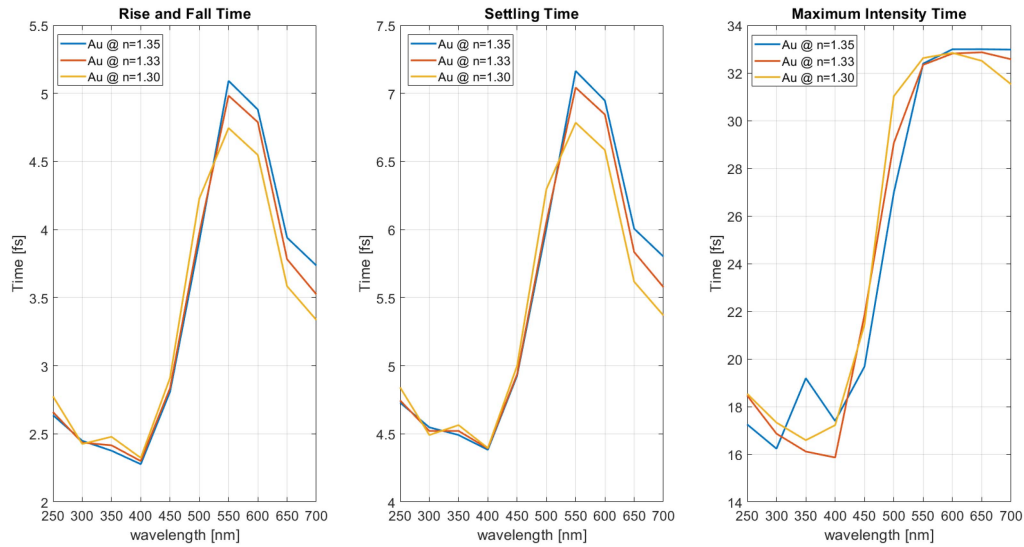
Fig. 5. Rise, fall, settling and maximum intensity time for several wavelengths and analyte's refractive indexes.

For low wavelengths, the number of photons at the steady state tends also to decrease, until gets closer to other gold resonances at ultraviolet regions.

Moreover, the nanoantenna response presents sensitivity to this refractive index variation at the SPP resonances. In other words, the number of extraordinary photons on the target will be dependent on the analyte's refractive index and consequently, it might work as a sensor.

It is also possible to compute the rise and fall times as well as the settling and the maximum intensity time stamps. The rise and fall times are defined as the time interval between the response reaching 10% and 90% of its maxima. The settling time corresponds to the time at which the optical response does not vary more than 10% of its steady-state value (maximum intensity, in this case). Furthermore, the maximum intensity time is the first time stamp in which the optical response reaches its maximum value. Fig. 5 presents the evolution of these results as a function of the wavelength.

The dependence of the rise and fall time with the analyte's refractive index is neglectable, within the gold resonances. In contrast, for high wavelengths, the response times present clear variations. It is due to the fact that for wavelengths higher than the resonances', the metal reflects all the radiation and consequently, it only propagates inside the analyte and the semiconductor substrate. Consequently, the time variations are due to the different propagation velocities in the media. Thus, responses for different analyte's refractive index have similar results since they only differ in the photons' velocity in the analyte, which is quite similar (small refractive index variation).

On the other hand, as already verified in Fig. 4, the response in resonant wavelengths has twice the intensity from the previous ones. Consequently, the response is quite dependent on the photons that pass through the metal and for that reason, it reaches its maximum at half the time.

Regarding the settling time, the results in Fig. 5 suggest that different analytes led to different settling times within the resonant wavelength. The settling time variation with the wavelength

has the same shape as the rise and fall time. In the resonant wavelengths, the propagation velocity within gold is higher than in the semiconductor or in the analyte. Thus, the more photons that pass through the metal, the lower the rise, fall and settling times will be.

Then main conclusion from the maximum intensity time stamp analysis is that the response reaches its maximum value at the end of the excitation (near 33 fs), but this value drops by half within the resonant wavelengths.

In Fig. 6 are the steady state values for the ten responses in the range between 250 nm and 700 nm. Once again, the device is only sensitive to the refractive index variation within the gold SPP resonances. Furthermore, the maxima sensitivities appear around 350 nm and 450 nm.

The device response at high wavelengths gold SPP resonances tends to the null sensitivity. Moreover, since metal reflects all the radiation, its complex electrical permittivity does not influence the response besides the consequence of giving the total reflection. Then, all the photons that reach the target have similar optical paths, travelling the same distances at the same time intervals, as also verified in Fig. 2. For that reason, the sensitivity at high wavelengths does not depend on the referenced refractive index, for instance taking similar values from 1.30 to 1.33 and from 1.33 to 1.30. This is presented in Fig. 7 where are the six sensitivities obtained by combining the results from the three analysed refractive indexes, where the sensitivity from the refractive index a to b is defined as $S_{a \rightarrow b} = \frac{(|N_a - N_b|)/N_a}{|a-b|} \times 100$ [%/RIU], being $N_{a,b}$ the number of photons detected on the target.

As expected from previous figures, the maximum sensitivity to measure variations between 1.30 and 1.33 is at 350 nm. Regarding the analysis between 1.30 and 1.35, the maximum is obtained for 450 nm, but the sensitivity at 350 nm also presents similar values. Both are around 90-100%/RIU. At 450 nm there is also the highest sensitivity, determined for the variation between 1.33 and 1.35, which takes values around 110%/RIU. This is the refractive index variation that presents the highest global
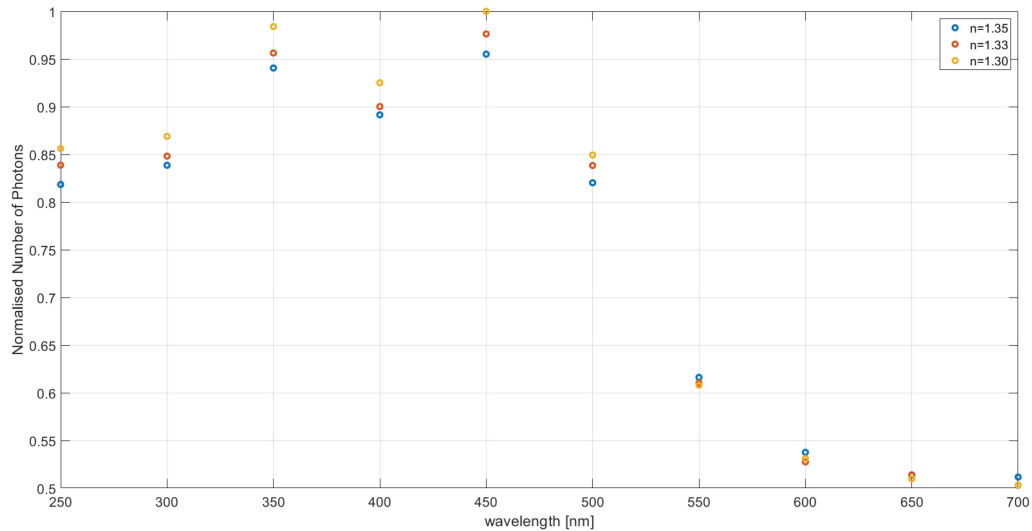
Fig. 6. Normalised steady state number of photons for several wavelengths and analyte's refractive indexes.
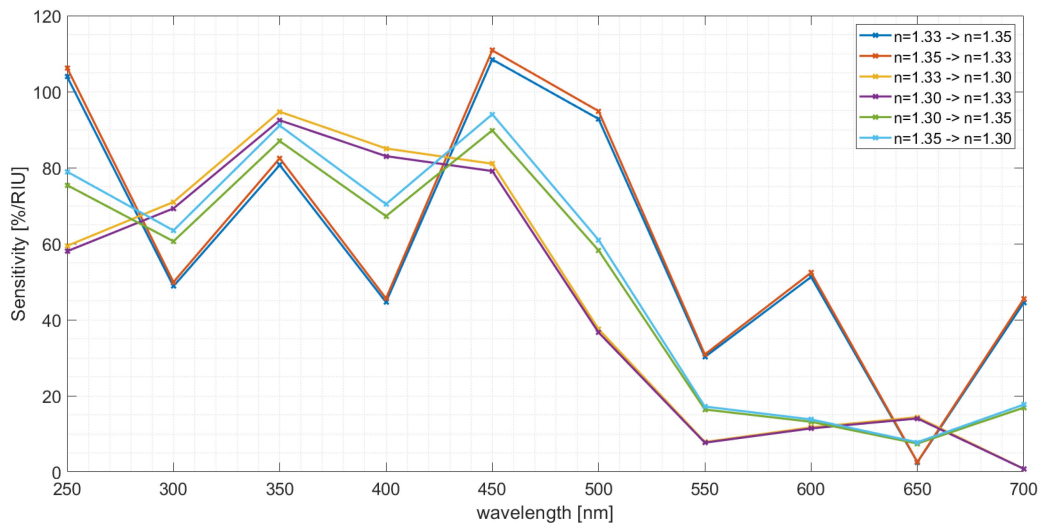

Fig. 7. Device sensitivity considering the analyte's refractive index combinations as function of the wavelength.

sensitivity and the highest sensitivities at the red spectral region. However, in the other visible wavelengths it leads to the lowest values. Also, it generates the highest sensitivity comparing the values at 250 nm (ultraviolet and near a gold resonance), taking a value near the global sensitivity maximum.

IV. DISCUSSION

In contrast with classical theories, it is verifiable that radiation in the optical range may pass through metallic nanolayers, due to the propagation of Surface Plasmon Polaritons. Thus, more intense beams are obtained when using plasmonic nanoslits (nanoantennas), near the SPP resonances. Once the metals' complex electric permittivity varies with the incident wavelength, the way metals may transmit or reflect energy also varies with it. In reality, it depends on both media in a certain interface. Then, sensors may be designed considering this phenomenon. This is

not possible to do outside metals' SPP resonances since in those conditions their electric permittivity is high enough, reflecting all the incident radiation independently on the other medium's permittivity.

Some of the metals that have this plasmonic behaviour in the optical range are gold, silver, platinum, copper and aluminium. In this case, to measure refractive index variation around 1.33, gold is the most indicated since is the one whose complex electric permittivity varies closer to the symmetric of that value [3].

The presented graphics are normalised to the maximum number of photons in the target. To detect a certain variation, one may have a reference and, for that reason, the measured quantity should be some difference between the analysed and the reference signal. For instance, in this case, one may emit at the maximum sensitivity wavelength and save as a reference the target power for a known analyte's refractive index. Only after that, one may monitor the analyte. This is quite an important

statement because if one emits a high-power optical signal, such as the emission Poissonian distribution tends to the uniform distribution, the higher the emitted power is, the higher the difference between signals.

The biggest advantage of having a slit nanoantenna instead of just a continuous metallic layer is that there is always a minimum number of photons reaching the target, namely the ones that pass directly through the slits (first peak observed in Fig. 2). Then, radiation is concentrated after the nanoantenna, considering photons from the slits and from the metal. Furthermore, the existence of vertical and horizontal metal-dielectric or metal-analyte interfaces allows the variation of its angle of incidence. It may bring some benefits because usually, the reflectance values are high for large incident angles and low for small ones, or vice-versa.

V. Conclusion

First, it is evident that near SPP resonances light is twice more intense than the obtained at higher wavelengths, considering the steady state number of photons. This is verified not only in the obtained pulse responses but also in the traced spectra.

The variation of light intensity in the target is dependent on the media due to the SPP resonances. For that reason, this research work aims to analyse a sensor based on a gold nanoantenna, exploiting EOT, by considering the previous statement as the device's working principle.

From the obtained results it is concluded that analysis at 350 nm and 450 nm are the best to monitor refractive index variations within 1.30 and 1.35. The highest sensitivity is at 450 nm to detect a variation from 1.33 and 1.35. However, the analysis at 350 nm also presents an excellent commitment. The global sensitivity maximum is around 110%/RIU, taking values around 80–90%/RIU in the visible spectral region.

Comparing the values within the 250–500 nm range with the ones outside it, one may conclude that the sensor's working principle is based on EOT, being SPP the main agents of this phenomenon. Also, the propagation of SPP allows the achievement of high sensitivities and only near the metals' resonances the device is capable of monitoring the proposed variations.

References

[1] T. Ebbesen, H. Lezec, H. Ghaemi, T. Thio, and P. A. Wolff, "Extraordinary optical transmission through sub-wavelength hole arrays," *Nature*, vol. 391, pp. 667–669, 1998, doi: 10.1038/35570.

[2] P. Lalanne and H. Liu, "The elementary interactions in the extraordinary optical transmission phenomenon," *J. Phys.: Conf. Ser.*, vol. 139, no. 1, 2008, Art. no. 012001, doi: 10.1088/1742-6596/139/1/012001.

[3] R. A. M. Lameirinhas, J. P. N. Torres, A. Baptista, and M. J. M. Martins, "A new method to analyse the role of surface plasmon polaritons on dielectric-metal interfaces," *IEEE Photon. J.*, vol. 14, no. 4, Aug. 2022, Art. no. 2236409, doi: 10.1109/JPHOT.2022.3181967.

[4] R. A. Marques Lameirinhas, J. P. N. Torres, A. Baptista, and M. J. M. Martins, "A new method to determine the response of Kretschmann's structure-based biosensors," *IEEE Sensors J.*, vol. 22, no. 21, pp. 20421–20429, Nov. 2022, doi: 10.1109/JSEN.2022.3207896.

[5] R. A. M. Lameirinhas, J. P. N. Torres, A. Baptista, and M. J. M. Martins, "A novel analysis for light patterns in nano structures," *IEEE Photon. J.*, vol. 14, no. 6, Dec. 2022, Art. no. 2763406, doi: 10.1109/JPHOT.2022.3227429.

[6] R. A. Marques Lameirinhas, C. P. C. V. Bernardo, J. P. N. Torres, A. Baptista, and M. J. M. Martins, "Analysis of a plasmonic slit nanoantenna as a high sensitivity tilt sensor," *IEEE Sensors J.*, vol. 23, no. 17, pp. 19232–19238, Sep. 2023, doi: 10.1109/JSEN.2023.3296270.

[7] R. A. Marques Lameirinhas, J. P. N. Torres, A. Baptista, and M. J. M. Martins, "The impact of nanoantennas on ring resonators' performance," *Opt. Commun.*, vol. 490, 2021, Art. no. 126906, doi: 10.1016/j.optcom.2021.126906.

[8] E. Purwandari, A. Arkundato, L. Rohman, and B. E. Cahyono, "Analyses of concentration and wavelength dependent refractive index of sugar solution using sellmeier equation," *J. Phys.: Conf. Ser.*, vol. 1825, 2021, Art. no. 012030, doi: 10.1088/1742-6596/1825/1/012030.

[9] D. Z. Stupar et al., "Remote monitoring of water salinity by using side-polished fiber-optic U-shaped sensor," in *Proc. 15th Int. Power Electron. Motion Control Conf. Expo.*, 2012, pp. LS4c.4-1–LS4c.4-5, doi: 10.1109/EPEPEMC.2012.6397458.

[10] M. F. H. Arif et al., "Photonic crystal fiber based sensor for detecting binary liquid mixture," *Opt. Photon. J.*, vol. 07, pp. 221–234, 2017, doi: 10.4236/opj.2017.711020.

[11] T. A. Oyehan, I. O. Alade, A. Bagudu, K. O. Sulaiman, S. O. Olatunji, and T. A. Saleh, "Predicting of the refractive index of haemoglobin using the hybrid GA-SVR approach," *Comput. Biol. Med.*, vol. 98, pp. 85–92, 2018, doi: 10.1016/j.compbiomed.2018.04.024.

[12] E. N. Lazareva and V. V. Tuchin, "Measurement of refractive index of hemoglobin in the visibleNIR spectral range," *J. Biomed. Opt.*, vol. 23, no. 3, 2018, Art. no. 035004, doi: 10.1117/1.JBO.23.3.035004.

[13] D. Fu, W. Choi, Y. Sung, Z. Yaqoob, R. R. Dasari, and M. Feld, "Quantitative dispersion microscopy," *Biomed. Opt. Exp.*, vol. 1, pp. 347–353, 2010, doi: 10.1364/BOE.1.000347.

[14] J. Liu et al., "Selecting temperature for protein crystallization screens using the temperature dependence of the second virial coefficient," *PLoS One*, vol. 6, 2010, Art. no. e17950, doi: 10.1371/journal.pone.0017950.

[15] P. S. Pandey, S. K. Raghuwanshi, and S. Kumar, "Recent advances in two-dimensional materials-based Kretschmann configuration for SPR sensors: A review," *IEEE Sensors J.*, vol. 22, no. 2, pp. 1069–1080, Jan. 2022, doi: 10.1109/JSEN.2021.3133007.

[16] R. Boruah, D. Mohanta, A. Choudhury, P. Nath, and G. A. Ahmed, "Surface plasmon resonance-based protein bio-sensing using a kretschmann configured double prism arrangement," *IEEE Sensors J.*, vol. 15, no. 12, pp. 6791–6796, Dec. 2015, doi: 10.1109/JSEN.2015.2464675.

[17] P. S. Pandey, S. K. Raghuwanshi, A. Shadab, M. T. I. Ansari, U. K. Tiwari, and S. Kumar, "SPR based biosensing chip for COVID-19 diagnosis–A review," *IEEE Sensors J.*, vol. 22, no. 14, pp. 13800–13810, Jul. 2022, doi: 10.1109/JSEN.2022.3181423.

[18] M. S. Rahman, M. S. Anower, M. R. Hasan, M. B. Hossain, and M. I. Haque, "Design and numerical analysis of highly sensitive Au-MoS2-graphene based hybrid surface plasmon resonance biosensor," *Opt. Commun.*, vol. 396, pp. 36–43, 2017, doi: 10.1016/j.optcom.2017.03.035.

[19] S. Zangenehzadeh et al., "Bacteria detection in a Kretschmann geometry flow cell at a plasmon-enhanced interface with spectroscopic ellipsometer," *Thin Solid Films*, vol. 764, 2023, Art. no. 139583, doi: 10.1016/j.tsf.2022.139583.

[20] M. K. Alam, M. U. Zaman, N. R. Alqhtani, A. Robaian, A. S. Algahtani, and A. Alrahlah, "Bismuth telluride, graphene, and silver based surface plasmon resonance biosensor for dental application," *Opt. Quantum Electron.*, vol. 55, no. 5, 2023, Art. no. 474, doi: 10.1007/s11082-023-04703-1.

[21] J. Pitarke, V. Silkin, E. Chulkov, and P. Echenique, "Theory of surface plasmons and surface plasmon polaritons," *Rep. Prog. Phys.*, vol. 70, no. 1, 2006, doi: 10.1088/0034-4885/70/1/R01.

[22] S. Zhang, L. Liu, and Y. Liu, "Generalized laws of snell, fresnel and energy balance for a charged planar interface between lossy media," *J. Quantitative Spectrosc. Radiative Transfer*, vol. 245, 2020, Art. no. 106903, doi: 10.1016/j.jqsrt.2020.106903.

[23] P. C. Y. Chang, J. G. Walker, and K. I. Hopcraft, "Ray tracing in absorbing media," *J. Quantitative Spectrosc. Radiative Transfer*, vol. 96, no. 3/4, pp. 327–341, 2005, doi: 10.1016/j.jqsrt.2005.01.001.

[24] M. N. Polyanskiy, "Refractive index database," Accessed: Dec. 26, 2022. [Online]. Available: https://refractiveindex.info

[25] P. A. D. Gonçalves et al., "Plasmon–emitter interactions at the nanoscale," *Nature Commun.*, vol. 11, 2020, Art. no. 366, doi: 10.1038/s41467-019-13820-z.